USING FLUX BALANCE ANALYSIS TO PREDICT METHYL-MERCURY PRODUCTION BY SULFATE REDUCING BACTERIA

by

SWETHA KUMAR KASETTY

Thesis submitted to the

Graduate School-New Brunswick

Rutgers, The State University of New Jersey

In partial fulfillment of the requirements

For the degree of

Master of Science

Graduate Program in

Environmental Science

Written under the direction of

A.J. Both and Tamar Barkay

And approved by

_____

_____

_____

_____

New Brunswick, New Jersey

October 2017

ABSTRACT OF THE THESIS

USING FLUX BALANCE ANALYSIS TO PREDICT METHYL-MERCURY PRODUCTION BY SULFATE REDUCING BACTERIA

by SWETHA KUMAR KASETTY

Thesis Director:

Dr. A.J. Both

Mercury (Hg) is a heavy liquid metal with high volatility. Elemental mercury can be transported around the globe and cause environmental and health problems. The primary anthropogenic sources of Hg in our atmosphere are from mining and burning fossil fuels. When Hg from the atmosphere gets deposited on the earth's surface, microorganisms biotransform it into methylmercury. Methylmercury (Me-Hg) is a potent neurotoxin and can bioaccumulate through aquatic food chains. A simulation model that can predict Me-Hg production by microorganisms could improve quantification and potentially aid in developing management strategies. Me-Hg production is carried out by anaerobic microorganisms and dependent on the molecule bound to Hg. Working with Hg can be very challenging and for these reasons measuring production rates is time consuming and requires the use of

sophisticated equipment. Studies have shown that sulfate-reducing bacteria are the major contributors in the production of Me-Hg. The sulfate-reducing micro-organism *Desulfovibrio desulfuricans* ND132 was used to study the rates of Me-Hg when exposed to different Hg (II) concentrations. ND132 is an organism with a hypothesized metabolic pathway for Hg methylation and was used to determine Hg methylation kinetics. Based on lab studies with pure cultures of ND132, a flux balance, a mathematical approach for analyzing the flow of metabolites through a metabolic network, was developed. The model attempted to predict Hg methylation rates for pure culture samples and Me-Hg concentrations for environmental samples. The simplified simulation model could help with rapid quantification and hence faster management and remediation of harmful mercury emissions.

Acknowledgement

I would like to extend my deepest gratitude to my advisors Dr. A.J. Both and Dr. Tamar Barkay and my committee members Dr. John Reinfelder and Dr. Jeffra Schaefer for all their help and guidance throughout my years as a graduate student. I would like to thank Philip Sontag and Cindy Wang for their help with all the lab work needed for my project. I would also like to thank Tanvi Borkar and Ajay Ramakrishnan for their help and expertise with the computer programming.

I want to thank my family for always encouraging me to follow my love for biology. I send a big heart-felt thank you to all my friends. My life is never boring because of you people! Lastly, I would like to thank the Department of General Biology for providing me with funding for my three semesters as a graduate student.

Table of Contents

List of Figures

List of Tables

Chapter 1

Literature Review

1.1. Mercury

Mercury (Hg) is a heavy, d-block (periodic table) element (atomic number 80) and the only metallic element that is liquid at standard temperature and pressure. This chemical element can be found throughout the environment. It is considered highly toxic (classified as a neurotoxin) because it can accumulate in the food web (bioaccumulation), and eventually affect human health. Despite its toxicity, Hg is still in use in different devices, including fluorescent lamps and some batteries, it is also used in artisanal gold mining in parts of the developing world (Clarkson and Magos, 2006; Steckling et al., 2017)

Hg can exist as elemental Hg (Hg (0)), inorganic Hg (Hg (I) and Hg (II)) and various organic forms (e.g., Me-Hg, Et-Hg) in the environment. Hg (II) is the dominant form of Hg in water, soil, and sediment while methylmercury (Me-Hg) and Hg (0) are the major species in higher trophic level biota and atmosphere, respectively. All forms of Hg are highly toxic to organisms. (Fitzgerald and Clarkson, 1991)

1.2. Introduction to the mercury cycle

Certain forms of Hg like Hg (0) are circulated globally causing health and environmental hazards making it a global pollutant (Tchounwou et al., 2012). The primary anthropogenic sources of Hg in the atmosphere result from: 1) artisanal gold mining in which gold is extracted using primitive techniques (Hg is used to bind to the gold in the ore and smelting the amalgam releases Hg and leaves gold; Steckling et al., 2017) and 2) Burning of fossil fuels, coal in particular. Coal itself does not contain large concentrations of Hg, however it is the amount of coal that is burned that contributes to high volumes of Hg being released into the environment (Pacyna et al., 2006). Natural sources of Hg include emissions from volcanic eruptions and geothermal vents. Hg cycles between the atmosphere, water and soil. It is deposited onto the surface both by wet-deposition (through precipitation) or dry-deposition (particulates settling out of the atmosphere; includes accumulation of elemental Hg by plant leaves) and these depositions of Hg from the atmosphere can lead to its biotransformation to Me-Hg (Amodio et al., 2014).

The Hg cycle starts with the release of elemental mercury (Hg (0)) through anthropogenic or natural sources into the atmosphere in vapor form (Figure 1). Once in the atmosphere, elemental Hg vapor can disperse over large distances and may have a residence time for up to a year. In the atmosphere, Hg is abiotically oxidized to Hg (II), a water-soluble form, and is deposited onto the surface of the Earth (Morel et al., 1998). Once this oxidized mercury reaches

an anaerobic environment such as bottom waters, lakebeds, wetlands or other waterlogged areas (Fitzgerald et al., 1998; Gosar 2006; Gray et al., 2014), it can potentially be converted into methyl-mercury (Me-Hg). Anaerobic microbes predominantly carry out this process enzymatically (Gilmour et al., 2013). Me-Hg then enters water bodies where it bio-magnifies by aquatic food chains and eventually can reach the human consumers of fish (Kim and Zoh, 2012; Barkay et al., 2003). Figure 1 shows how mercury is transformed and mobilized in the environment.

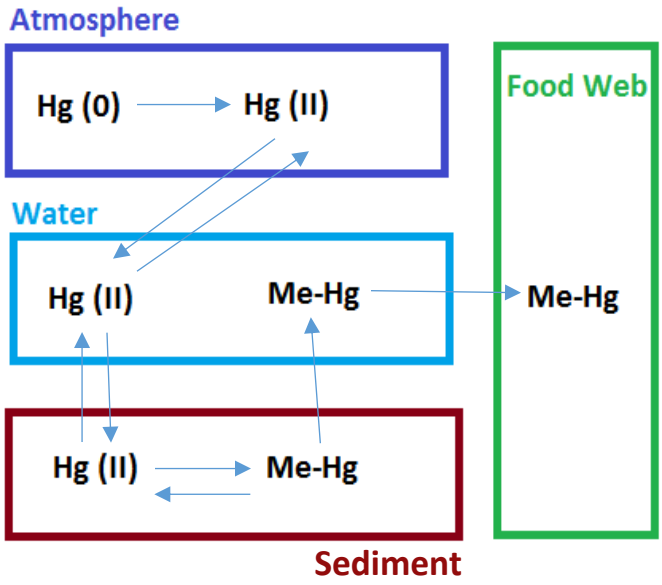

Figure1. Partial mercury cycle showing mercury transformation and transport in the environment, including into methyl-mercury and eventual uptake and bioaccumulation by living organisms.

1.3. Methyl-mercury: Toxicity

Awareness about the detrimental effects of Me-Hg arose in the 1960s following a toxicosis episode in Minamata Bay, Japan, as the result of consumption of Me-Hg contaminated fish (Harada, 1995). As mentioned earlier, Me-Hg is a potent neurotoxin that can bio-accumulate in the food chain. The two groups that are most at risk from adverse effects of methylmercury exposure are women of childbearing age and children who consume freshwater fish. In fetuses, methylmercury interferes with cell division and cell migration causing neurobiological defects. It has been shown to cause problems with memory, attention, language skills, visual-motor skills and a general decrease in higher-order cognitive functions (Hong, Kim & Lee, 2012). Adults with increased levels of methylmercury in their system have been known to develop paresthesia (typically a burning sensation in extremities). Long term exposure to low concentrations of methylmercury increases the risk of contracting myocardial infarction and coronary heart disease (Diez, 2008).

1.4. Microbial conversion of mercury to methyl-mercury

Microbial methylation of mercury (Hg) is one of the major contributors to public health concern with Hg pollution. Inorganic Hg (II) is converted to Me-Hg enzymatically (Parks et al 2013) solely by anaerobic microorganisms in habitats like saturated soils, wetlands and sediments (Fitzgerald et al., 1998; Gosar 2006; Gray et al., 2014; Gilmour et al., 2013; Pak and Bartha, 1998). That living organisms methylate Hg (II) was first discovered by Jensen and Jernelo (1969),

who showed that in anoxic aquariums and lake sediments, Hg (II) was methylated, and that this activity was inhibited by sterilization.

Studies with pure cultures have shown sulfate-reducing bacteria (SRB) are the major contributors (Compeau & Bartha, 1985) although strains of iron-reducing bacteria, methanogens, fermenters, and dehalogenating bacteria also are involved in the production of Me-Hg (Gilmore et al., 2013). Methylation is specified by the *hgcA* and *hgcB* genes with *hgcA* encoding for a coronoid-binding protein responsible for the methylation of Hg (II) and *hgcB* an electron donor required for corrinoid cofactor reduction (Parks et al., 2013). The metabolic pathway that includes *hgcAB* genes are still unknown, while Choi et al. (1994) suggested a link between *hgcAB* genes to Acetyl Co-A pathway. Ekstrom et al. (2003) proposed the possibility of a second metabolic pathway in SRB not capable of using Acetyl-CoA pathway.

1.5. Mercury availability and uptake

Initially it was speculated that Hg uptake into the cell was through passive diffusion across the cell membrane. However, not all Hg present is available to the microorganisms, Schaefer et al. (2011) have shown that microbial cells could take up Hg (II) when complexed to thiols and enters the cell through ligand exchange in sulfide free solutions. Hg complexed with thiols in natural organic matter along with Hg complexes with FeS minerals and two forms of cinnabar has also been known to be bioavailable to micoorganisms in anoxic sediments (Jonsson et al.,

2012). For SRB sulfide is likely to limit methylation by the formation of insoluble mercuric sulfide (making it unavailable for microbial uptake). It was therefore hypothesized that methylation occurs at a range of sulfate concentrations below which SRB respiration is inhibited and above which excessive sulfide is produced (Gilmour and Henry, 1991; Benoit et al., 1999). Although Hg speciation does not directly have an effect on Hg methylation, it is likely it influences the fate and transport processes of Hg. One possible method to eliminate the transportion process to study methylation kinetics is to provide excess of the thiol groups to ensure all the Hg is in a form available for uptake For ND 132, the organism used for experiments in this project, Hg complexed to glutathione showed maximum Hg methylation (Schaefer et al., 2011).. Further, Schaefer et al. (2014) hypothesized that Hg (II) transport into the cell could be an outcome of accidental uptake during the procurement of essential trace metals like Zn (II). Once inside the cell, Hg (II) is methylated in the cytosol and the Me-Hg is exported out of the cell (Schaefer et al., 2011).

1.6. Metabolic pathway for mercury methylation

Choi et al. (1994) laid the foundation to the discovery of the metabolic pathway involved in biological-mercury methylation in anaerobes. *Desulfovibrio desulfuricans* LS was chosen as the model organism due to its high methylating rates. Using radioisotope studies, the path of carbon was tracked and it was concluded that the methyl group originated from formate via the Acetyl-CoA pathway or from C-3 of serine. They further measured the activities of enzymes involved and proposed a metabolic pathway (Figure 2).

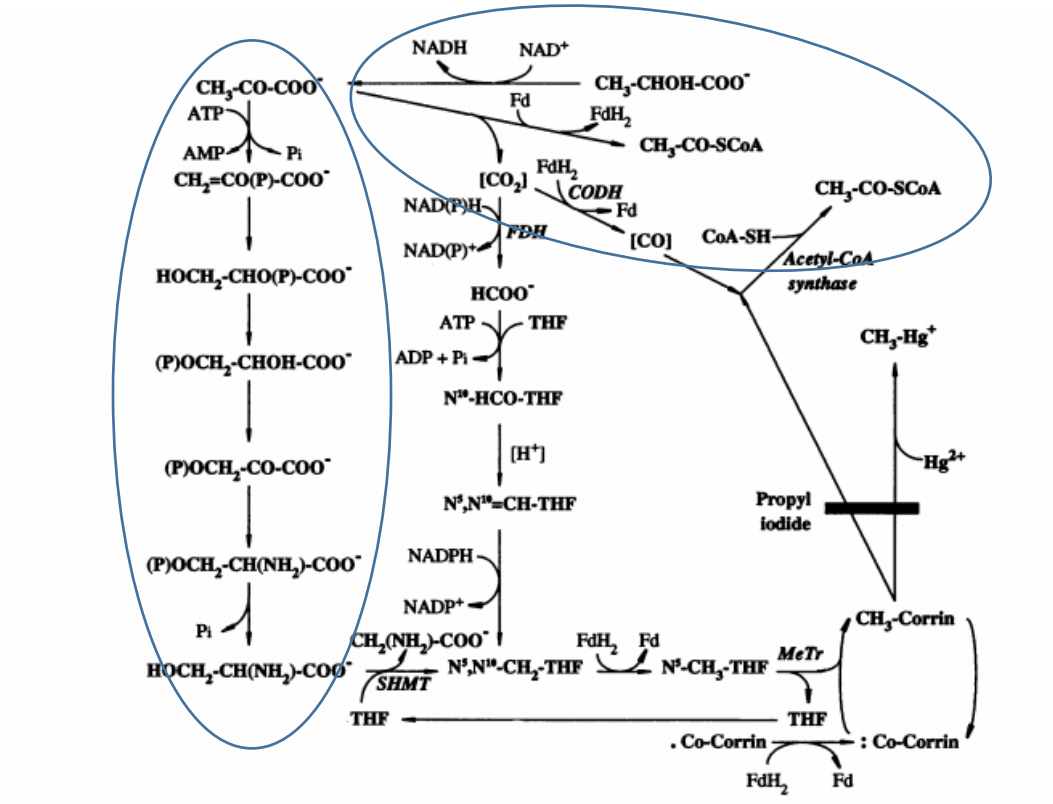

Figure 2. Metabolic pathway suggested by Choi et al. (1994) for mercury methylation in *Desulfovibrio desulfuricas LS.* The Acetyl-CoA pathway (top-right) and the serine biosynthesis pathway (left) have been circled.

We now know all methylating strains carry the *hgcA*/*hgcB* genes (Parks et al., 2013) and thus, it seems that any differences in the methylation pathways is due to tetrahydrofolate (THF), the major methyl donor to Hg (II) in methylation. The pathways connecting THF to *hgcAB* may be different in different organisms or the THF fluxes may be different leading to different methylation rates. The diversity of the biochemical pathways that methylate mercury are still largely unknown, and further studies are required.

1.7. Mercury Demethylation

The reverse process of Hg methylation simultaneously occurs in sediment and wetlands where methylation occurs. Unlike Hg methylation which is restricted to some subsets of microorganisms, MeHg demethylation is more wide spread (Hines et al., 2006). Research shows that Me-Hg degradation can follow two distinctive paths (Oremland et al., 1991) oxidative and reductive, the latter being associated to mercury resistance *(mer)* operon (Barkay et al., 2003). In some environments production of Me-Hg is typically higher its degradation, leading to a net accumulation of Me-Hg (Gilmour et al., 1998). Kronberg et al (2012) have shown high demethylation rates limiting Me-Hg concentration. The accumulation of Me-Hg is thus reflective of the balance between relative rates of Hg methylation and demethylation

1.8. Mercury-methylation and Temperature

Previous research and recent studies support a positive correlation between Me-Hg production rates and temperature implying warmer temperatures could promote microbial Hg methylation (Bacci, 1989; Bodaly et al., 1993; Monperrus et al., 2007). Recent studies on the impacts of global climate change have focused on the changes in the Hg biogeochemistry in the Arctic region. Since the impacts of temperature increase are already being experienced in the Arctic (Douglas et al., 2012; Stern et al., 2012), there have been several studies examining the impact of warming on ecosystems (Jansson and Tas, 2014; Yang et al., 2016). These studies have demonstrated that increase in temperature promotes the release of Hg (II) that has been sequestered in the environment (Gordon et al., 2016). These changes, together with increased microbial activity as a

result of warmer temperatures, have been hypothesized to result in greater rates of methylation and Me-Hg bioaccumulation in the Arctic (Podar et al., 2015; Yang et al., 2016). For these reasons, the relationship between methylation rate and increasing temperatures requires further study. Data reported in one of the few studies that investigated the impact of change in temperature on methylation (Mauro et al., 1999) has been used in the work described here.

1.9. Mercury methylation and pH

Prior studies demonstrated that the highest levels of methylation were typically associated with acidic environments (Ramlal et al., 1986; Bloom et al., 1991; Gilmour and Henry, 1991; Gilmour et al., 2013), recent studies have observed methylation to occur in lakes with a neutral pH (Correia et al., 2012) and in prairie alkaline wetlands with a pH exceeding 8 (Hoggarth et al., 2015; Gilmour et al., 2013). Nevertheless, the precise effect of pH on Hg methylation is yet unclear and more studies are required. Data reported in one of the few studies that investigated the impact of pH on methylation (Mauro et al., 1999) has been used in the work described here.

1.10. *Desulfovibrio desulfuricans* ND 132 as a model organis

Cindy Gilmour and her group have expanded our understanding of methylation and de-methylation of Hg by microorganisms by characterizing *D. desulfuricans* ND 132 (ND 132) in detail providing a model organism for Hg methylation (Gilmour et al., 2011). The same organism

was chosen for this study of Hg methylation because it exhibited exceptionally high rates of Me-Hg production but otherwise appeared to be a relatively typical anaerobic strain. Its 16s DNA sequence showed that it was close relative to the LS strain used by Choi et al (1994) (Gilmour et al., 2011) (The LS strain is lost to science). The organism has a wide range of salt and pH tolerance. Unlike many SRB strains, ND132 has the ability to grow well using fumarate as an alternative electron acceptor to sulfate, allowing the study of methylation during rapid growth while avoiding sulfide inhibition of methylation by making Hg unavailable for uptake, a common challenge during the study of methylation (Gilmour et al., 2011). ND 132 was used in this study to characterize Hg methylation kinetics in the presence of excess glutathione which ensures uniform Hg speciation and allows for maximal rates without problems associated with Hg bioavailability. In addition, the complete genome for ND 132 is available and will allow comparison with the many available full-genome sequences of other *Desulfovibrio* spp, other SRB and FeRB strains, and present an opportunity for studies that might include comparative transcriptomic and proteomic studies.

1.11. Flux Balance Analysis

Flux balance analysis (FBA) is a widely used approach for studying biochemical networks. These network reconstructions contain all of the known metabolic reactions in an organism and the genes that encode each enzyme. FBA calculates the flow of metabolites through this metabolic network, thereby making it possible to predict the growth rate of an organism or the rate of production of an important metabolite (Orth et al., 2011).

The Michaelis-Menten (M-M) model is one method that can be used to track the flux of metabolites through a biochemical pathway. The M-M model is one of the simplest and best-known approaches to study enzyme kinetics. It relates the enzyme reaction rate to substrate concentration for a reaction or system where a substrate *S* binds reversibly to an enzyme *E* to form an enzyme-substrate complex *ES*, which then reacts irreversibly to generate a product *P* and to regenerate the free enzyme *E*. This system can be represented schematically as follows:

$$E + S \leftrightarrow ES \rightarrow E + P$$

(Equation 1)

The M-M equation for this syste$m\ is$:

$$V = Vmax[S]/(Ks + [S])$$

(Equation 2)

Here, V_{max} represents the maximum reaction rate achieved by the enzyme, at saturation substrate concentrations. K_s (the Michaelis constant) is the substrate concentration at which the reaction rate is 50% of the V_{max}. [*S*] is the concentration of the substrate *S* (Roskoski, 2015).

In general, the solution obtained by FBA is only as good as the constraints used to build the model. Therefore, it is very important to invest a lot of time and effort in a quality

reconstruction of metabolic networks, including the selection of constraints. FBA focuses only on part of whole genome metabolic pathway utilizing enzymes and their kinetics, which catalyse the various metabolic reactions in the cell.

1.12. Future Directions

Knowledge about Hg bioavailability to microorganisms and the different pathways involved in Hg methylation is one of the key steps to predict Me-Hg concentrations in different environmental compartments. Although significant positive correlations have been found between time and Me-Hg concentrations in many environments (Drott et al., 2008), these short-term measurements of potential rates of methylation and demethylation have been found to be unrelated to gross measures of long-term Me-Hg accumulation (Drott et al., 2008; Johnson et al., 2016). More studies are required to establish a relationship between short-term and long-term Me-Hg accumulation.

The most significant discovery in mercury methylation research recently has been the discovery of the *hgcAB* gene cluster, which is necessary for methylation (Gilmour et al., 2013; Parks et al., 2013). This developing area of research is likely to enable significant strides in the future by identifying biota that possess methylating capacities, the environments that these organisms can inhabit, and by extension, which environments may be at risk of Me-Hg contamination.

Chapter 2

Materials and Methods

2.1 Experimental methods and errors

Parameters such as initial concentration of the analytes, sample composition, storage materials and other conditions (e.g., light, temperature, and pH) usually affect the stability of Hg converting species and should be monitored as much as possible. The risk of contamination due to minor impurity or contamination of the sampling materials, additives, and the storage containers should be avoided. In addition, some forms of Hg are either volatile, have strong affinity for surface adsorption and/or leak into or out of storage materials which can affect the original sample composition.

2.2. Microorganisms and Culture Conditions

The sulfate reducing bacterium, *Desulfovibrio desulfuricans* ND132 was obtained from the Gilmour laboratory (C.C. Gilmour, Smithsonian Environmental Research Center). Strain ND132 was initially grown in a modified medium for *Desulfovibrio vulgaris* (Zane et al., 2010) with lactate (60 mM) as the electron donor and sulfate (30 mM) as the acceptor at 30 °C. One week prior to the experiments ND 132 was grown on 25 mM pyruvate and 30 mM fumarate in a low-sulfate medium modified from a previously described medium (Ekstrom et al., 2003) containing (pH 7.3) 10 mM Mops, 1.5 mM KH_2P0_4, 4.7 mM NH_4Cl, 6.7 mM KG, 3.2 mM $MgCl_2$, 1.4 mM

$CaCl_2$, 257 mM NaCl, 25 µM Na_2S0_4, 23 nM Na_2Se0_3, 24 nM Na_2W0_4, 3.6 uM $FeCl_2$, 1 mg/L resazurin and 1 mL/L of a sulfate-free SL-7 trace metal solution adapted from one previously described (Widdel and Pfennig, 1981). All media were boiled, allowed to cool while bubbling with 0_2 free N_2 gas, dispensed into acid-cleaned serum bottles, sealed with rubber stoppers, and autoclaved.

2.3. Mercury Methylation Experiments

Hg uptake and methylation assays were prepared under strict anoxic conditions in 20 ml_ acid-cleaned serum bottles assay buffer containing 1m M of each electron acceptor/donor pair in which the cells were grown (fumarate and pyruvate). The assay buffer was free of sulfate and contained 10 mM Mops, 0.1 mM NH4Cl, 0.5 mM KCl, 0.4 mM $MgCl_2$, 0.2 mM KH_2P0_4, 170 mM NaCl, 1 mM pyruvate, 1 mM fumarate, and 1 mg/L resazurin (Schaefer et al., 2011).Hg methylation assays were conducted in serum bottles containing 15 ml assay buffer and sealed under anoxic conditions (N_2 headspace) with Teflon stoppers. Prior to the start of the methylation experiments, 10 µM glutathione was added to each assay vial and allowed to equilibrate with different concentrations of inorganic mercury (II) (0.05, 0.5, 1, 5, 10 and 50 µM) (3 samples at each Hg concentration) in 15 mL of assay buffer in a Teflon stoppered serum bottle for two hours at 30 °C. To assess the extent of abiotic methylation during distillation, assay bottles containing buffer, 10 µM glutathione and Hg (II) but no cells were acidified and also distilled (A total of 6 samples; 3 with low Hg (II) concentration = 1.5 µM and 3 with high Hg (II) concentration = 75 µM).

All manipulations of the strain during the washing procedure were performed in an anaerobic chamber (Coy Laboratory Products, Inc., Grass Lake, MI) under a gas mixture of 97% N_2 and 3% H_2 (supplied by Airgas®). Cells were harvested during the exponential phase of their growth curve, centrifuged for 7 minutes at 7400 xg, washed three times in fresh assay buffer and then re-suspended in the same assay buffer to an optical density of 0.2 at 660 nm (OD_{660}). The corresponding protein concentration of a cultures with an OD_{660} of 0.02 was 38 ng protein/ml considering that OD_{660} of 1 = 1.9µg protein/ml (Wang, personal communication). Aliquots of washed cells (1 ml) were then added to the assay vials to arrive at a final density (OD_{660}) of 0.02. Cells were then incubated with Hg (II) for two hours at 30°C. Hg methylation was stopped by freezing at -20°C the entire contents of individual bottles. Bottles from all experiments remained frozen until Me-Hg analysis.

2.4. Methyl-mercury Analysis

Samples were distilled prior to methyl-mercury analysis using a Tekran® 2750 gas manifold and heating unit (Tekran® Instruments Corporation, Toronto, ON, Canada) according to EPA method 1630 (EPA Method 1630: Methyl Mercury in Water by Distillation, Aqueous Ethylation, Purge and Trap, and CVAFS, EPA 821-R-01-020, United States Environmental Protection Agency, January 2001). The only modification made to the distillation procedure was the addition of cupric sulfate (1 M) in place of 1% Ammonium pyrrolidinedithiocarbamate (APDC) to mitigate interferences from remnant sulfide in the mixture (Olson et al., 1997) Three distillation blanks were evaluated and all were below 0.4 pM and Me-Hg concentration spike recoveries were

within EPA guidelines (110 ± 5.5%, n = 3). Distilled samples were derivatized using aqueous phase ethylation (Bloom, 1989) and analyzed by gas chromatography coupled to cold vapor atomic fluorescence spectroscopy (GC–CVAFS) on a Tekran® 2700 (Tekran® Instruments Corporation, Toronto, ON, Canada).

2.5. Total Mercury Analysis

For total Hg analysis, 5 mL aliquots were removed from each replicate assay and placed into acid cleaned Teflon digestion vials. Samples were oxidized using bromine monochloride (BrCl), at a final concentration of 0.01 N. Total Hg analysis was performed at least 24 h after BrCl addition. Samples were diluted in ultrapure water and excess BrCl was neutralized using 2 M hydroxylamine hydrochloride prior to sample introduction. Mercury analysis was performed using tin chloride (0.45 M) reduction followed by cold vapor atomic absorption spectroscopy (CVAAS) on a Hydra AA (Teledyne-Leeman Laboratories, Hudson, NH). Procedural blanks were all below 0.1 nM Hg.

2.6. Methyl-Mercury Calculator/ Simulation Model

For the simulation model, the Me-Hg metabolic pathway was simplified using limiting reactions as can be seen in Figure 3. The K_s and V_{max} of enzymes involved in the reactions were obtained from the literature and are listed in Table 1.

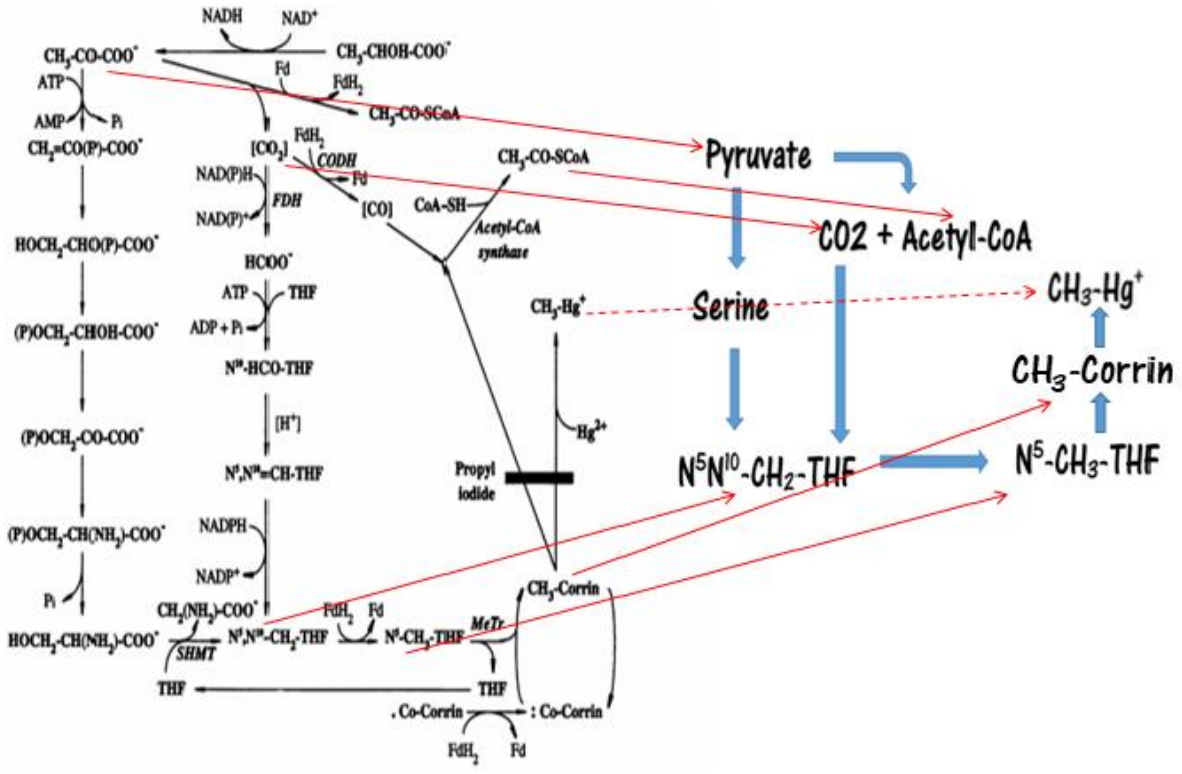

Figure 3. Metabolic pathway for mercury methylation by *D. desulfuricans LS* (Choi et al., 1994). Arrows point to corresponding metabolites in the simplified mercury-methylation pathway used for the flux balance (shown on the right).

Enzyme kinetics equations were used to predict the rate of change from one metabolite to the next. Reactions 1-6 shown in Figure 4 were assumed to conform to the first order Michaelis-Menten equation (i.e., the rate of conversion of a substrate depends on the substrate concentration) and Equation 2 was used to model conversions of substrates to products. Reaction 2 (Figure 4) has a very small V_{max}, implying that the serine pathway was slower than the Acetly-CoA pathway. For this reason reactions 1 and 2 were excluded from the model. Other reaction rates decrease: V3 > V4 > V5 (Table 1), and thus reaction 5 is the rate limiting

step. The pyruvate concentration, an input value supplied by the model user, is used as substrate concentration to estimate the rate of reaction according Equation 1 using the K_s and V_{max} of reaction 5 (Table 1). Since V6 > V5, the steady-state approximation ($d[N^5\text{-}CH^3\text{-}THF]/dt = 0$; V5=V6) was used to estimate the concentration of $N^5\text{-}CH^3\text{-}THF$. It was assumed that the $N^5\text{-}CH^3\text{-}THF$ concentration is equal to the CH_3-Corrin concentration. Since TFH is the methyl carrier I assumed that all of the methyl groups are transferred to the Corrin molecule making their concentrations equal. In addition kinetics for CH_3-Corrin is still unavailable. Equation 3, the MM equation for two substrate enzymes, was then used to find the rate of Me-Hg production based on the concentrations CH_3-Corrin from the biochemical model and of Hg (II) that is provided as input by the model user. Since K_s values of the *hgcA* and *hgcB* protein is still unavailable, they were estimated from experimental rate measurements by substituting values from experimental data into the two substrate MM equation to obtain the K_s of the *hgcA* and *hgcB* protein.

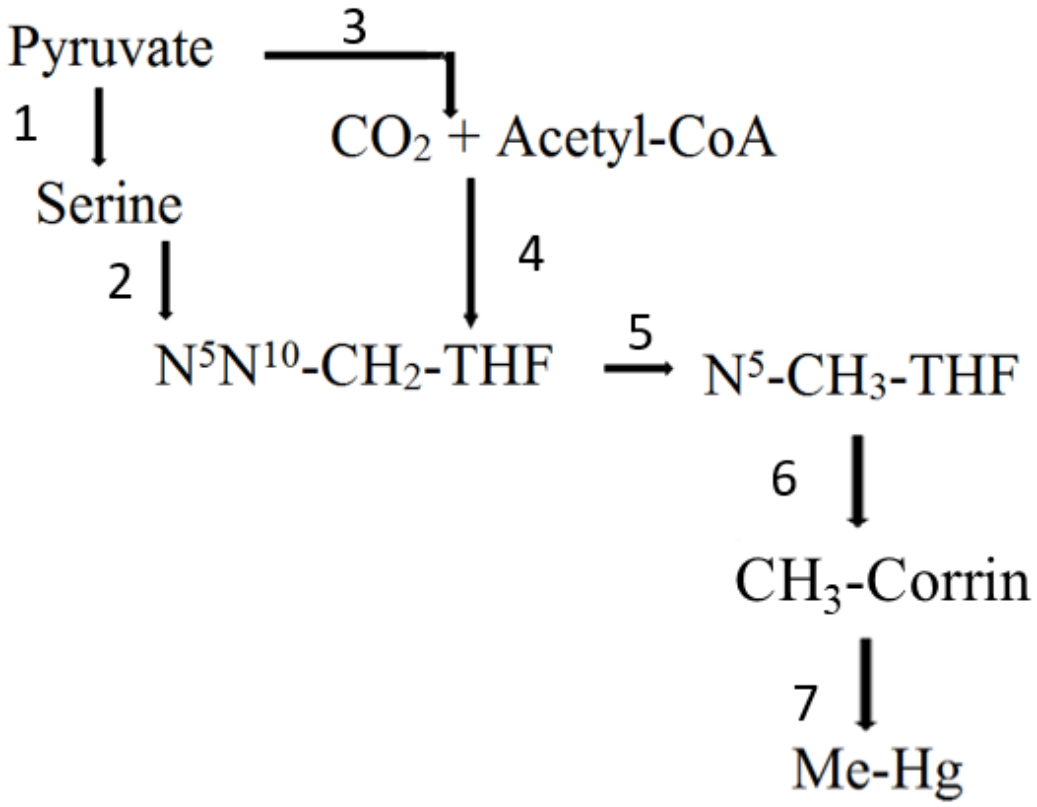

Figure 4. Simplified mercury-methylation pathway used to predict Methyl-mercury production rates. The numbers indicate the different limiting reactions in the simplified pathway. Kinetic data used from Kushkevych, 2015 (Reaction 1); Choi et al., 1994 (Reaction 2, 4 and 5); Diender et al., 2015 (Reaction 3); Menon and Ragsdale, 1999 (Reaction 6).

$$V = Vmax\,[S1][S2] / (Ks2[S1] + Ks1[S2] + [S1][S2])$$

(Equation 3)

Here V_{max} is the maximal velocity with both S_1 and S_2 saturating, K_{s1} is the concentration of S_1 that gives ½ V_{max} when S_2 is saturating, K_{s2} is the concentration of S_2 that gives ½ V_{max} when S_1 is saturating (Roskoski, 2015).

Since Hg uptake by the cell depends on Hg speciation, the environmental conditions of the cell will change the uptake and hence V_{max} at different external conditions for the cell. The substrate concentration (S_1) and substrate concentration at ½ V_{max} (K_{s1}) for Hg (II) were determined from the experimental data for glutathione conditions. The V_{max} and K_s values used in the model are listed in Tables 1 and 2.

Two conditions in addition to Hg methylation in the presence of glutathione were included in the model: methylation in sulfate reducing conditions and methylation in environmental samples (Hg (II) bound to natural organic matter). This study is based on incubation of estuarine sediment samples with different Hg (II) concentrations. For these two conditions, corresponding linear equations were utilized in the model (Table 2).

Table 1. Lists of V_{max} and K_s values used for the Me-Hg prediction model. The equation numbers relate to those in the simplified Me-Hg metabolic pathway (Figure 4). References: Kushkevych, 2015 (Reaction 1); Choi et al., 1994 (Reaction 2, 4 and 5); Diender et al., 2015 (Reaction 3); Menon and Ragsdale, 1999 (Reaction 6).

Reaction No. (Figure 4)	Enzyme	V_{max} (µM of substrate min^{-1} mg^{-1} protein)	K_s µM
1	Pyruvate dehydrogenase	0.89	2550
2	Serine hydroxymethyltransferase	0.042	0.116
3	Acetyle CoA synthase	1.6	9
4	Carbon monoxide dehydrogenase	0.178	10
5	Methylene-THF dehydrogenase	0.011	0.290
6	Methyltransferase	0.22	10
7	HgcA and HgcB protein	NA	0.13 Apparent K_s calculated with the model

Table 2. List of V_{max} and K_s values used in the methyl-mercury prediction model for methylation under different conditions.

Condition (Reference)	V_{max} (µM of substrate min^{-1} mg^{-1} protein)	K_s µM
Glutathione (From experiment)	5.515E-6 (Calculated from Lineweaver-Burk Plot)	0.018 (Calculated from Lineweaver-Burk Plot)
Sulfate (Gilmour et al., 2011)	NA Me-Hg = 3 log (Hg (II)) (Concentration; 32h incubation time; 0.4-0.6 OD at 660nm)	NA
Environmental Samples (Jansson et al., 2014) (Hg (II) bound to natural organic matter)	NA Me-Hg=0.0489 Hg(II) +1.22 (Concentration/gram sediment; 7 day incubation time)	NA

In addition to the above conditions, methylation rates as a function of temperature and pH were determined from Mauro et al. (1999). Polynomial and linear fits were performed which yielded four equations. Their experiments provided information about the percentage of Me-Hg produced as a function of temperature or pH. Unfortunately, the exact concentrations of the Me-Hg were not provided. This information was converted into equations that were used in the model to predict Me-Hg concentrations at different temperatures and pH values as shown in Figures 5 and 6. The different equations used are listed in Table 3. Based on the reference temperature and pH of 30ºC and 7, respectively (temperature and pH at which the data was obtained), the percentages of Me-Hg production could be calculated for other temperatures and pH values as shown in Equation 4:

$$\text{Me—Hg Conc. At new temp} = \frac{\text{Relative \% Me—Hg at new temp} * \text{Me—Hg Conc. At 30˚C}}{\text{Relative \% Me—Hg at 30˚C}}$$

(Equation 4)

This calculation can be used only to the conditions that predict concentrations of Me-Hg that is produced. The concentration of bioavailable Hg (II) is also assumed to be the same at the changing pH and temperatures.

Table 3. List of different conditions and equations used for the mercury methylation prediction model. See Figures 5 and 6 for a graphical representation of these equations (based on Mauro et al., 1999).

Condition (x)	Type of Fit	Equation	R^2
Temperature	Linear	$y = 0.6786x - 6.6429$ $(10 \leq x < 32)$	0.9701
		$y = -0.7357x + 39.074$ $(32 \leq x \leq 50)$	0.9154
	Poynomial	$y = -0.0312x^2 + 1.9409x - 17.199$ $(10 \leq x \leq 50)$	0.9368
pH	Linear	$y = 2.8x + 16.9$ $(3 \leq x < 6)$	0.9561
		$y = 34$ $(6 \leq x < 7)$	1
		$y = -11x + 111$ $(7 \leq x \leq 8)$	1
	Polynomial	$y = -1.4107x^2 + 15.775x - 10.807$ $(3 \leq x \leq 8)$	0.7338

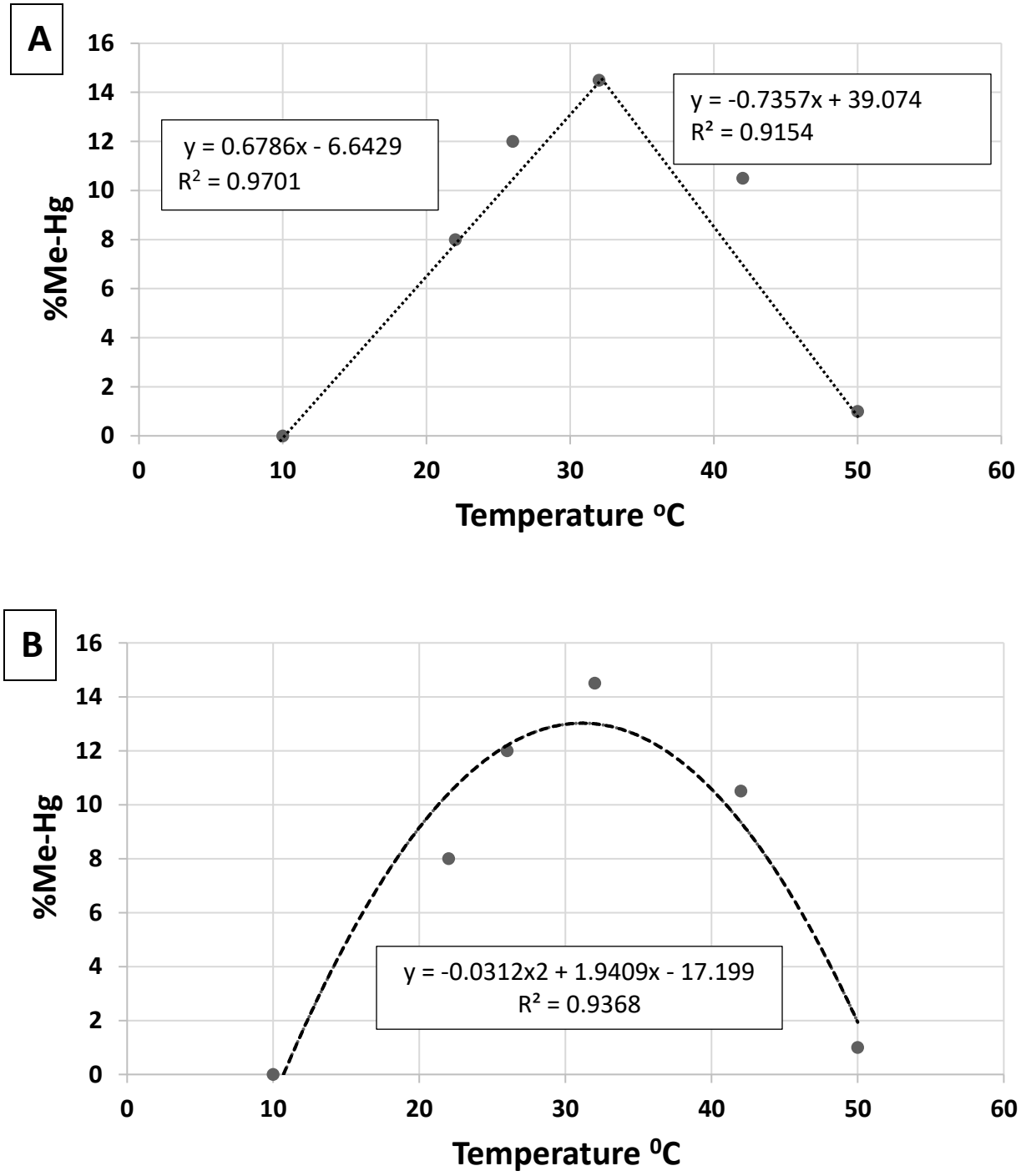

Figure 5. Graphs represent the linear (A) and polynomial (B) fits performed for effect of temperature on Hg methylation. Data obtained from Mauro et al., 1999.

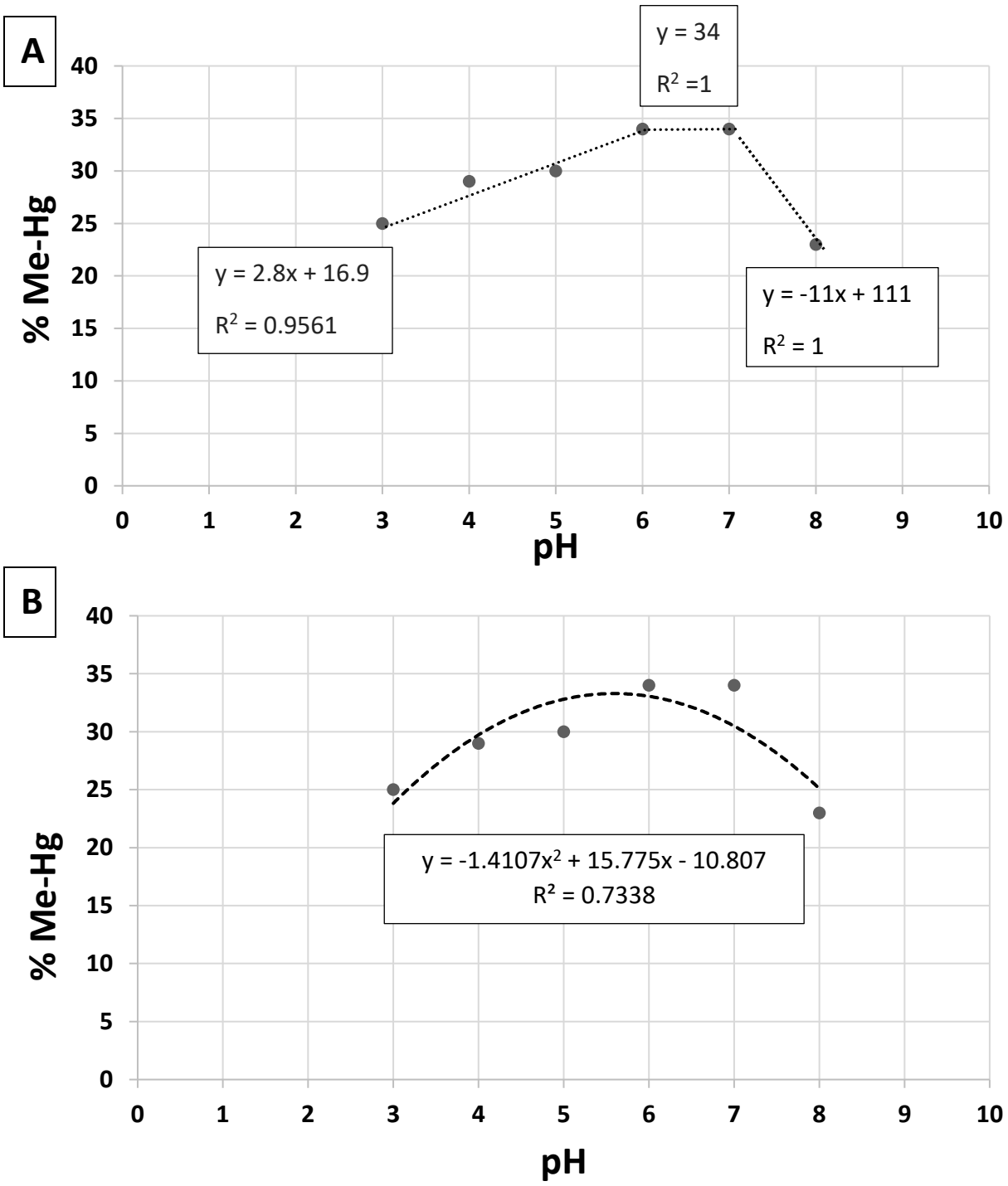

Figure 6. Graphs represent the linear (A) and polynomial (B) fits performed for effect of pH on Hg methylation. Data obtained from Mauro et al., 1999.

The following assumptions were for the model:

1. Concentration of pyruvate inside and outside the cell are equal
2. The pathway is not limited by THF
3. The serine pathway is always much slower than the CO_2 pathway and is ignored (Table 4 and Figure 2).
4. Since the rates decrease V3 > V4 > V5 (Table 4 and Figure 4), reaction 5 is the rate limiting step. The pyruvate concentration is used to calculate the substrate concentration to estimate the rate of reaction 5.
5. At steady-state, $d[N^5\text{-}CH^3\text{-}THF]/dt = 0$ and V5=V6)
6. At steady-state, substrate concentration of reaction 6 is equal to [CH3-Corrin]; $[N^5\text{-}CH_3\text{-}THF] = [CH_3\text{-}Corrin]$.
7. The concentration of Hg (II) (bioavailable) is the same at the changing pH and temperatures

Chapter 3

Results

3.1. Methyl-mercury production

Each vial used to measure methylation potential was amended with varying concentrations of Hg (II) and incubated for two hours at $30^{O}C$. Majority of the Hg (II) amendment levels substantial concentrations of Me-Hg compared to the uninoculated control assays. The final Me-Hg concentrations ranged from 0.37 ± 0.06 nM, when 0.01 µM Hg (II) was added, to 111.31 ± 15.5 nM of Me-Hg, when 303.18 ± 40.54 µM were added (Table 4). Although initial amendments of Hg (II) were calculated to achieve 0.05, 0.5, 1, 5, 10 and 50 µM Hg (II), a later analysis revealed large deviation from these targets. The actual Hg (II) amendments ranged between 0.01 and 303.18 ± 40.54 µM of Hg (II) (Table 4).

Table 4. The relationship of the concentration of Me-Hg produced by ND 132 to the concentrations of Hg (II) added to incubations. Amount of Hg (II) added to the buffer containing cell cultures is shown in the table. The abiotic controls have been shaded.

Actual amount of Hg (II) added, µM	Me-Hg produced, nM
0.01	-0.01
0.01	0.44
0.01	0.31
0.29	0.30
0.43	0.93
0.40	1.01
6.77	1.10
5.46	0.26
5.62	1.25
41.12	0.83
33.28	0.88
22.19	-0.10
78.69	0.78
89.14	12.16
93.99	8.10
294.67	111.31
258.33	73.53
356.55	95.85
Abiotic Controls	
1.5	79.45
1.5	188.57
1.5	39.58
1.5	124.22
1.5	81.08
75	69604.93
75	5366.47
75	3206.67
75	107238.19
75	113063.46

The results show that with an increase in Hg (II) concentration there is a linear increase in Me-Hg production as seen in Figure 7. Previously published research shows that the ND 132 cells grow at 80% of its normal growth rate at a concentration of 50µM Hg (II) and the cells grow at 10% of their normal growth rate at an addition of 500 µM Hg (II) (Gilmour et al., 2011). We speculated the possibility that methylation could be reduced or even completely stopped with decrease in growth rates caused by increase in Hg (II) concentrations. For this reason it was hypothesized that Me-Hg that is produced (see Table 4) when more than 50 µM of Hg (II) added may be attributed to artifact Me-Hg production during aqueous distillation.

The distillation procedure for the extraction of Me-Hg is simple, precise and results in detection of extremely low concentrations; however, it has the potential for artifact formation. This results from the action of natural organic matter on the inorganic Hg present in the sample at high heat. In all cases, the rate of methylation increases dramatically with increasing temperature, which can be an issue considering the samples are heated to a temperature of approximately 125^0C during distillation. The effect of pH varies with the type of organic material present but the pH is usually maintained at a constant value (Bloom et al., 1991). Cells and organic compounds present in the assay vials form a rich source of organic matter in the distillation process. This may result in artifact methylation of 0.005-0.01% of the inorganic Hg (Bloom et al., 1991). Table 5 shows the conversion percentages for Me-Hg.

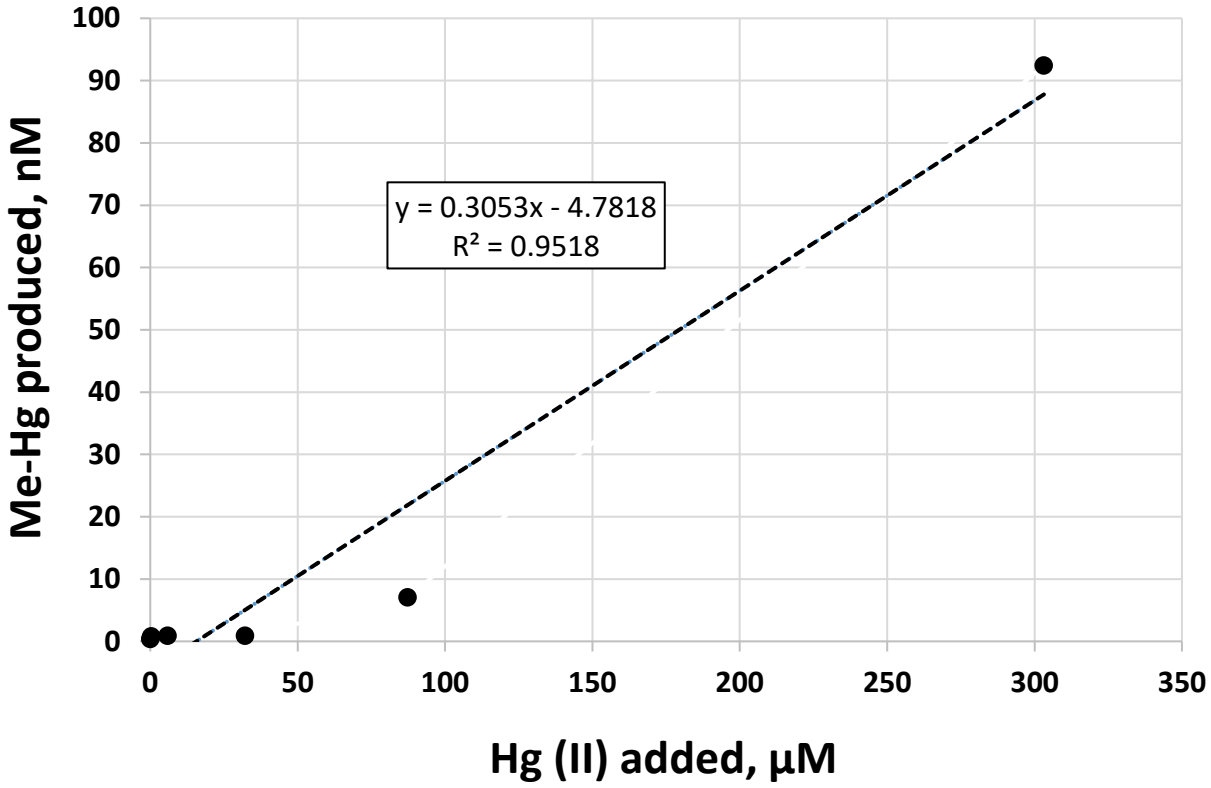

Figure 7. Me-Hg production as a function of different Hg (II) concentrations added to the media. The graph includes all Hg (II) concentrations used during the experiments. This culture of ND 132 was incubated for a time of 2 hours at 30^{O}C. The OD_{660} of the culture was 0.02 and incubations were carried out under excess glutathione conditions (10 µM).

Table 5. Percentage conversion of Hg (II) to Me-Hg in samples containing cell culture, buffer and Hg (II) amendments under excess glutathione conditions. The shaded region (gray) in the table represents likely artifact Me-Hg produced during distillation.

Amount of Hg(II) added, µM	Me-Hg, nM	%Me-Hg produced
0.01	-0.01	-0.069%
0.01	0.44	4.049%
0.01	0.31	3.814%
0.29	0.30	0.105%
0.43	0.93	0.217%
0.40	1.01	0.255%
6.77	1.10	0.016%
5.46	0.26	0.005%
5.62	1.25	0.022%
41.12	0.83	0.002%
33.28	0.88	0.003%
22.19	-0.10	0.000%
78.69	0.78	0.001%
89.14	12.16	0.014%
93.99	8.10	0.009%
294.67	111.31	0.038%
258.33	73.53	0.028%
356.55	95.85	0.027%

Further analysis of abiotic samples consisting of buffer and Hg (II) amendments supported the hypothesis showing that at high concentrations of Hg (II), 0.07% to 0.13% (Table 6) of Me-Hg was produced as a product of the distillation process. The assay buffer which contains pyruvate and fumarate along with glutathione is thought to be the source of organic matter in this case.

Table 6. Percentage conversion of Hg (II) to Me-Hg in abiotic samples containing buffer and Hg (II) amendments under excess glutathione conditions.

Conc. Of Hg(II) added, µM	Conc. Of Me-Hg produced, nM	% conversion
1.5	0.00	0%
1.5	0.17	0.01%
1.5	0.00	0%
1.5	0.00	0%
1.5	0.00	0%
75	55.64	0.07%
75	0.00	0%
75	0.00	0%
75	91.40	0.12%
75	96.52	0.13%

Excluding Hg (II) amendments above 75 µM in the experiment that was done with live cultures incubated for two hours (Table 4 and Figure 7), a curve (Figure 8) was obtained that shows Me-Hg production initially increases with an increase in Hg (II) concentration, reaches peak production and after that, there is a plateau in Me-Hg production until an addition of 32 µM of Hg (II).

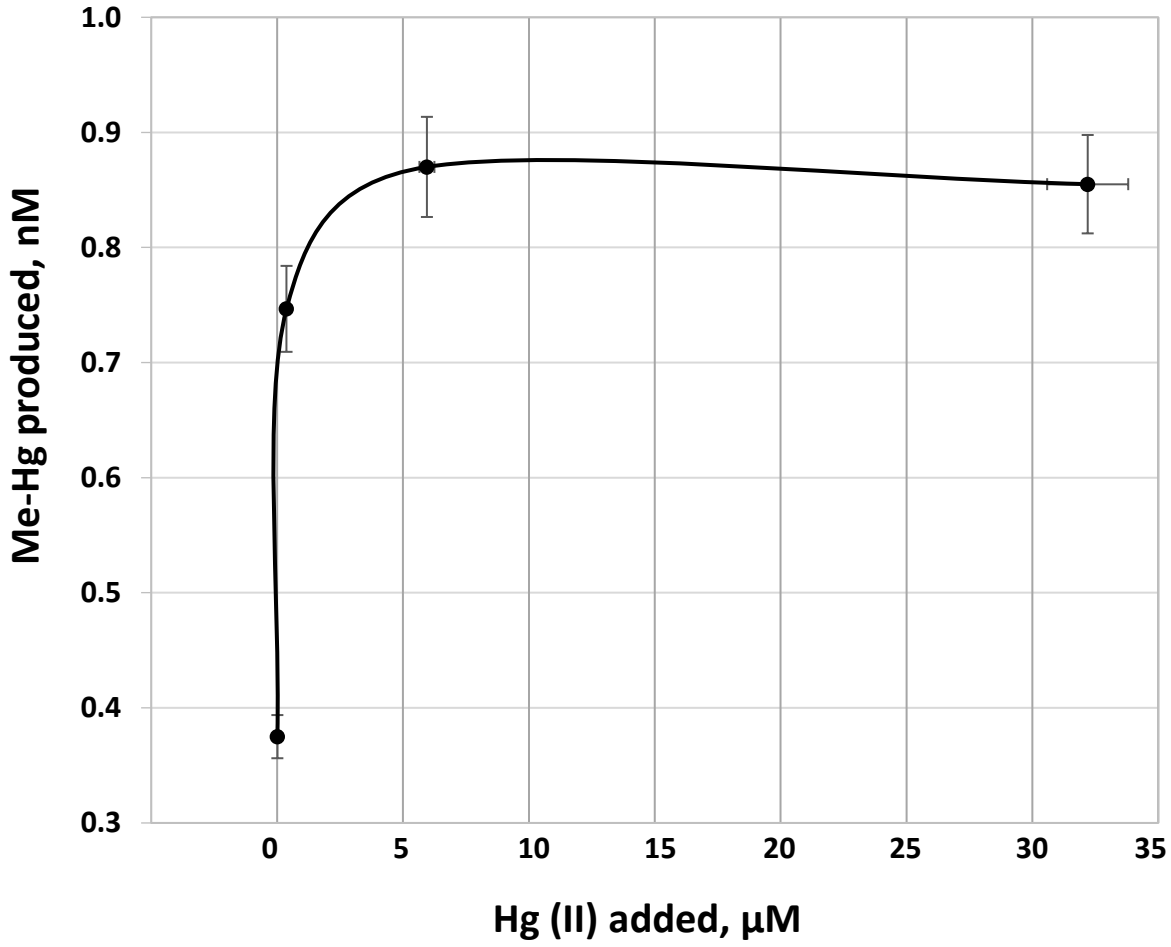

Figure 8. Me-Hg concentrations as a function of different Hg (II) concentrations added into the media. Replicate cultures of ND 132 with OD_{660} of 0.02 were incubated for 2 hours at $30^{O}C$ under excess glutathione conditions (10 µM).

The data was normalized assuming methylation to be a linear process (Jenssen et al., 2016), and Table 7 shows the normalization. The V_{max} was determined to be 5.515E-6 µM MeHg mg^{-1} protein h^{-1} and the half saturation concentration (K_s) of Hg (II) was calculated to be 0.018 µM using Lineweaver-Burk Plot (using data from Table 7) under excess glutathione conditions.

Table 7. Normalization of Me-Hg production data to obtain the maximum conversion rate of Hg (II) to Me-Hg under excess glutathione conditions.

Amount of Hg (II) Added, nM	Methylation rate, nmol/h	nmol MeHg mg^{-1} protein h^{-1}
10	0.1875	0.099 ± 0.0016
410	0.486	0.256 ± 0.01
6200	0.5865	0.309 ± 0.09
37200	0.4275	0.225 ± 0.07

3.2. Methyl-Mercury production calculator

A mathematical computer model was built using Hypertext Preprocessor (PHP) to predict methyl-mercury production by microbes using strain ND 132 as a test system. The interactive model allows the user to choose between different conditions and predicts Me-Hg produced at different temperatures and ranges of pH. The user can choose between ND 132 pure culture and environmental samples. When the pure culture is chosen, the user choses between glutathione or sulfate conditions, then enters concentration of pyruvate and Hg (II) added to

the media and the program predicts the concentration of Me-Hg generated and rate of methylation. Using environmental samples, the model attempts predict concentration of Me-Hg generated in sediment samples when Hg (II) is bound to natural organic matter; the user enters the concentration of Hg (II) to obtain predicted Me-Hg concentrations.

The model calculated a methylation rate of 4.42 pmol of Me-Hg min^{-1} mg^{-1} protein while Graham et al. (2012) showed the production rate to be 0.116 pmol of Me-Hg min^{-1} mg^{-1} protein for a Hg (II) concentration of 50 nM, the small increase in rate could be due to differences in Hg speciation. The model uses glutathione conditions while the study is conducted in cysteine conditions, we know that for ND 132 Hg methylation rate is higher in glutathione condition (Schaefer et al., 2011). The model 3.4 pmol of Me-Hg min^{-1} mg^{-1} protein while Janssen et al (2016) showed the production of 0.016 ± 0.002 nmol of Me-Hg min^{-1} mg^{-1} protein under cysteine conditions for a Hg (II) concentration of 40 nM. The stark difference in Hg methylation rates in the two studies. Further comparisons could not be conducted because of a lack of data. The environmental Me-Hg production rates also varied quite a bit when compared to work published by Heyes et al. (2006). The model predicted a production of 0.177 µmol of Me-Hg gram of $soil^{-1}$ day^{-1} whereas Heyes et al. (2006) reported values of 1.3 to 8.3 nmol of Me-Hg gram of $soil^{-1}$ day^{-1} both report Me-Hg concentrations with estuary sediments, however the model is limited and can predict Me-Hg concentrations only of Hg bound to organic matter. It cannot predict Me-Hg with changing sediment type, sediment depth or nutrient conditions.

3.3. Sensitivity analysis

A sensitivity analysis is a technique used to determine the effect of different values of independent variables on the output of a model. The analysis was conducted by changing one factor at a time. V_{max} and K_s values were changed one at a time by ±5 %, ±10, ±20 %, ±50%, ±75% and even +100% to determine how sensitive the model is and to which values. It was found that the output changed only by 0.05-0.9%, except when the K_s and V_{max} values for methylation in the presence of glutathione were changed, which resulted in a change of 0.9 to 2.8% in the output. The very small changes could in the output could be be attributed to: 1) The following step cancels out the effect of change from the preceding step, 2) the model is simulating only a small portion of the entire metabolic pathway, and 3) Model is not sensitive to changes in pyruvate concentration.

The concentration of Me-Hg increases linearly with the concentration of pyruvate, until the pyruvate concentration reaches 1 µM, after which increase in the pyruvate concentration does not affect the output. (The Hg (II) concentration constant).The model is more sensitive to changes in the input Hg (II) concentration suggesting very small concentrations of pyruvate is required for Hg methylation. It is important to note that the model does predict formation of Me-Hg at high Hg (II) concentrations.

A graph was created using calculations performed with the simulation model that shows how Hg methylation rates varied Hg (II) concentration (under a constant pyruvate concentration) for

the glutathione condition. A similar trend as shown in Figure 8 was observed: Me-Hg production initially increases with an increase in Hg (II) added, followed by peak production and a plateau in Me-Hg production (Figure 9).

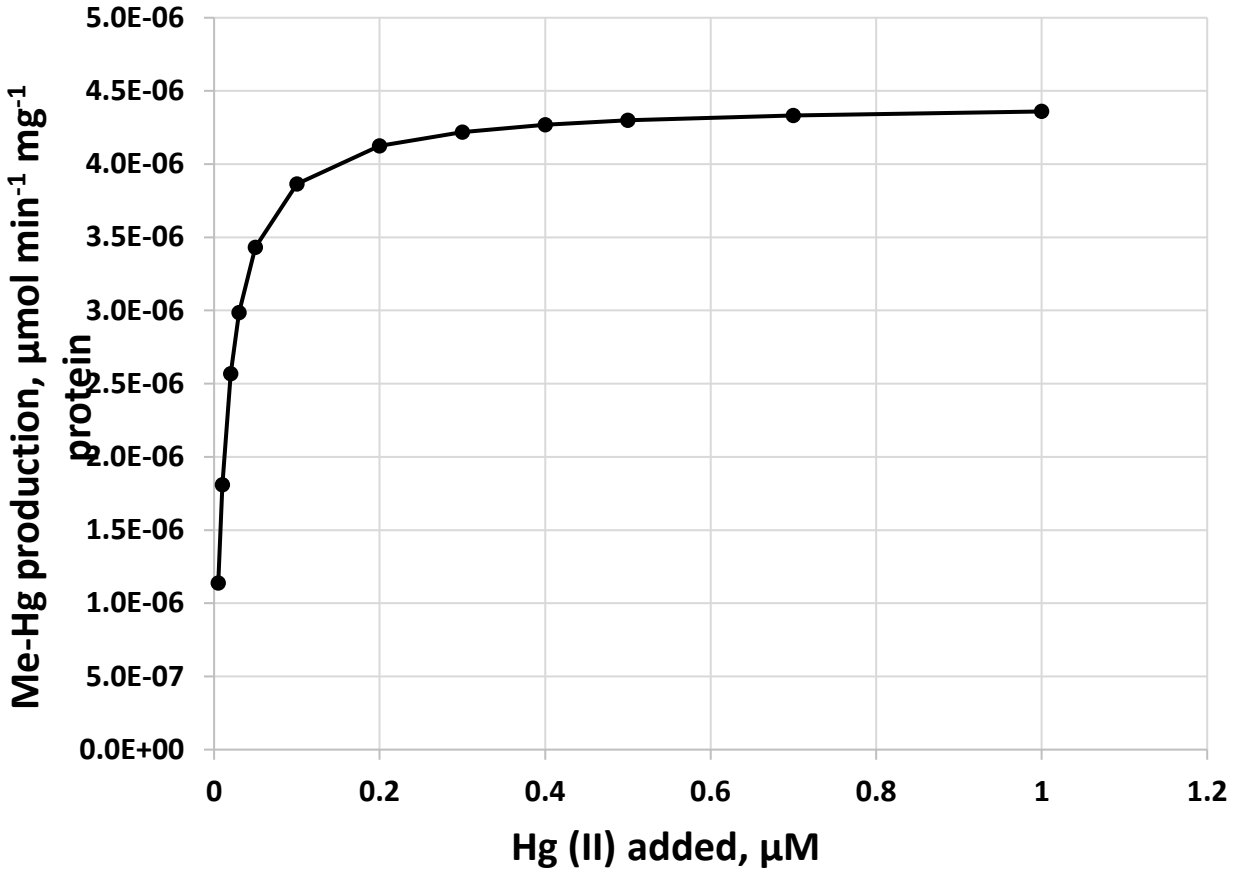

Figure 9. Predicted Me-Hg production rate as a function of different Hg (II) concentrations as calculated by the simulation model.

Another graph was created that compared the how close the model generated values were to the experimental values for the glutathione condition (Figure 10). A linear trend was observed with a R^2 value of 0.85. Since an R^2 of 1 implies the experimental and model generated values to be the same, more experimental data points could improve R^2 and make the model accurate.

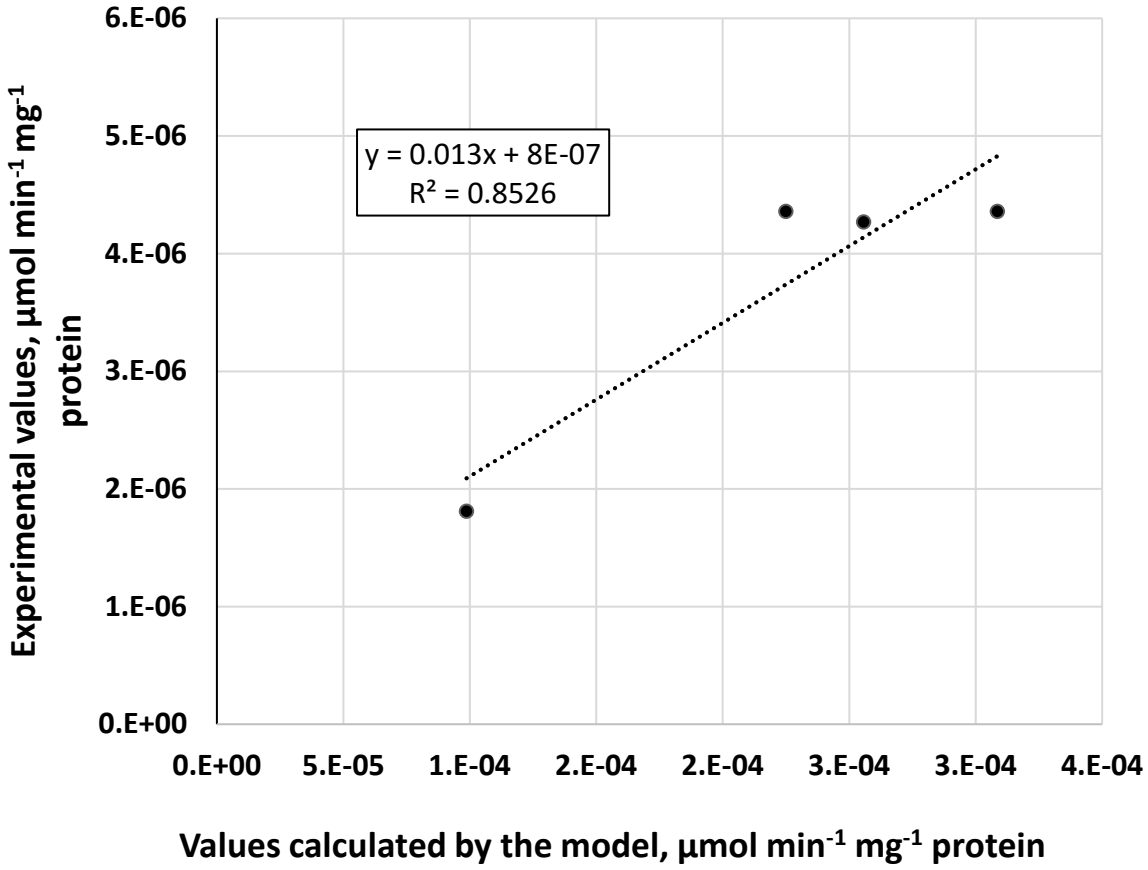

Figure 10: Comparing model generated and experimental Hg methylation rates for the excess glutathione condition.

Chapter 4

Conclusions and Future Directions

The kinetic model that was developed provides insight into the effects of Hg (II) concentration on Me-Hg production in the presence of excess glutathione. First, a steady increase in the Me-Hg production was observed, and then a peak production rate was obtained followed by a gradual decline in production rate. The apparent V_{max} was determined to be 5.515E-6 Me-Hg µM mg^{-1} protein h^{-1} and the K_s was 0.018 µM of Hg (II). Understanding and determining such kinetics data with different thiol complexes in the media or buffer, could help in determining Hg (II) uptake mechanisms in methylating organisms.

The accuracy and usability of the Me-Hg prediction model could be increased by conducting studies to determine the relationship between concentrations of pyruvate inside and outside the cell. The model assumes that both concentrations are the same. This seems unlikely and discovering the concentration of pyruvate actually entering the cell will make the calculations used in this model more accurate. Second, the proteins coded by *hgcAB* genes, which are directly involved in Hg methylation (Parks et al., 2013), are yet to be studied in detail. The knowledge of kinetic properties of these enzymes and the physical parameters that affect them will assist in making the Me-Hg prediction model more accurate. Third, Bioavailablity and Hg speciation are important controlling factors for Hg methylation. The model only calculates methylation for Hg bound to glutathione and Hg bound to natural organic matter. Other

bioavailable Hg species needs to be considered for the model to have border scale of usability. It is also important to note that the model uses bioavailable Hg (II) and not total Hg (II) in its working. Next, most studies measure the first order rate constant of Hg methylation in environmental samples (Jansson et al., 2014; Fitzgerald et al., 1998; Gosar, 2006), however for this model it is important to measure the half saturation constant of Hg methylation. It is also important to take into account demethylation rates while calculating the concentration of Me-Hg in environmental samples. Lastly, there is a lack of large data sets for model verification owing to the fact that this field of research is relatively new. The effect of binding Hg (II) to different ligands on its uptake is a recent discovery (Schaefer and Morel, 2009; Schaefer et al., 2011) and more kinetic studies can assist in making the Me-Hg prediction model more detailed especially for environmental samples.

The model was able to predict Me-Hg generated by different Hg (II) compounds, at temperatures and pH levels however, it faces several limitations. A simplified model like the one presented here could aid in rapid quantification of methyl-mercury production and could be first step required to extrapolate and determine the concentration of Me-Hg that could be harmful to the human population. Continued prediction and experimental verification is essential and integral part of the further development of model to use to represent methylation in its natural environment. The model could then lead to development of novel management strategies for the successful remediation of mercury emissions.

References

1. Amodio, M., Catino, S., Dambruoso, P., de Gennaro, G., Di Gilio, A., Giungato, P., Laiola, E., Marzocca, A., Mazzone, A., Sardaro, A. and Tutino, M. (2014). Atmospheric deposition: Sampling procedures, analytical methods, and main recent findings from the scientific literature. Advances in Meteorology, 1-27.

2. Bacci, E. (1989). Mercury in the Mediterranean. Marine Pollution Bulletin, 20(2):59–63.

3. Barkay, T., Miller, S. and Summers, A. (2003). Bacterial mercury resistance from atoms to ecosystems. FEMS Microbiology Reviews, 27(2-3):355-384.

4. Benoit, J., Mason, R., and Gilmour, C. (1999). Estimation of mercury-sulfide speciation in sediment pore waters using octanol-water partitioning and implications for availability to methylating bacteria. Environmental Toxicology And Chemistry, 18(10):2138-2141.

5. Bloom, N.S., Watras, C.J., and Hurley, J.P. (1991). Impact of acidification on the methylmercury cycle of remote seepage lakes. Water, Air, and Soil Pollution, 56:477–491.

6. Bloom, N.S. (1989). Determination of picogram levels of Methylmercury by aqueous phase ethylation, followed by cryogenic gas chrbomatography with cold vapour atomic fluorescence detection. Canadian Journal Of Fisheries And Aquatic Sciences, 46:1131-11.

7. Bodaly, R.A., Rudd, J.W.M., Fudge, R.J.P., and Kelly, C.A. (1993). Mercury concentrations in fish related to size of remote Canadian Shield lakes. Canadian Journal of Fisheries and Aquatic Sciences, 50:980–987

8. Choi, S., Chase Jr., T. and Bartha, R. (1994). Metabolic Pathways Leading to Mercury Methylation in Desulfovibrio desulfuricans LS. Applied and Environmental Microbiology, 60(11):4072-4077.

9. Clarkson, T., and Magos, L. (2006). The toxicology of Mercury and its chemical compounds. Critical Reviews In Toxicology, 36(8):609-662.

10. Compeau, G., & Bartha, R. (1985). Sulfate-Reducing Bacteria: Principal Methylators of Mercury in Anoxic Estuarine Sediment. Applied Environmental Microbiology, 50(2):498-502.

11. Correia, R.R.S., Miranda, M.R., and Guimarães J.R.D. (2012). Mercury methylation and the microbial consortium in periphyton of tropical macrophytes. Effect of different inhibitors. Environmental Research, 112:86–91.

12. Díez, S. (2008). Human health effects of methylmercury exposure. Reviews of Environmental Contamination and Toxicology, 198:111-132.

13. Douglas, T.A., Loseto, L.L., Macdonald, R.W., Outridge, P.M., Dommergue, A., and Poulain A. (2012). The fate of mercury in Arctic terrestrial and aquatic ecosystems, a review. Environmental Chemistry, 4:321-355.

14. Drott, A., Lambertsson. L., Björn, E., and Skyllberg, U. (2008). Do potential methylation rates reflect accumulated methyl mercury in contaminated sediments? Environmental Science & Technology, 42:153–158.

15. Ekstrom, E., Morel, F., and Benoit, J. (2003). Mercury methylation independent of the Acetyl-Coenzyme A pathway in sulfate-reducing bacteria. Applied And Environmental Microbiology, 69(9):5414-5422.

16. Fitzgerald, W., and Clarkson, T. (1991). Mercury and monomethylmercury: present and future concerns. Environmental Health Perspectives, 96:159-166.

17. Fitzgerald, W., Engstrom, D., Mason, R., and Nater, E. (1998). The Case for Atmospheric Mercury Contamination in Remote Areas. Environmental Science & Technology, 2(1):1-7.

18. Gilmour, C.C., and Henry, E.A. (1991). Mercury methylation in aquatic systems affected by acid deposition. Environmental Pollution, 71:131–169.

19. Gilmour, C.C., Podar, M., Bullock, A.L., Mitchell Graham, A., Brown, S., and Somenahally, A.C. (2013). Mercury methylation by novel microorganisms from new environments. Environmental Science & Technology, 47:11810–11820.

20. Gilmour, C.C., Elias, D., Kucken, A., Brown, S., Palumbo, A., Schadt, C., and Wall, J. (2011). Sulfate-reducing bacterium Desulfovibrio desulfuricans ND132 as a model for understanding bacterial Mercury methylation. Applied and Environmental Microbiology, 77:3938-3951.

21. Gilmour, C.C., Riedel, G.S., and Ederington. (1998) Methylmercury concentrations and production rates across a trophic gradient in the northern Everglades. Biogeochemistry, 40:327–345.

22. Gordon, J., Quinton, W., Branfireun, B.A., and Loefeldt, D. (2016). Mercury and methylmercury biogeochemistry in a thawing permafrost wetland complex, Northwest Territories, Canada. Hydrological Processes, 30(20):3627–3638.

23. Gosar, M. (2006). Mercury in river sediments, floodplains and plants growing thereon in the drainage area of the Idrija mine, Slovenia. Chinese Journal Of Geochemistry, 25(S1):34-34.

24. Graham, A., Bullock, A., Maizel, A., Elias, D., and Gilmour, C. (2012). Detailed assessment of the kinetics of Hg-cell association, Hg methylation, and Methylmercury degradation in several Desulfovibrio species. Applied And Environmental Microbiology, 78(20):7337-7346.

25. Gray, J., Hines, M., Goldstein, H., & Reynolds, R. (2014). Mercury deposition and methylmercury formation in Narraguinnep Reservoir, southwestern Colorado, USA. Applied Geochemistry, 50:82-90.

26. Harada, M. (1995). Minamata disease: Methylmercury Poisoning in Japan Caused by Environmental Pollution. Critical Reviews In Toxicology, 25(1):1-24.

27. Hines, Mark E., Jadran, F., Isaac, A., and Milena H. (2006). Microbial Mercury transformations in marine, estuarine and freshwater sediment downstream of the Idrija Mercury Mine, Slovenia". Applied Geochemistry 21 (11):1924-1939.

28. Hoggarth, C.G.J., Mitchell, C.P.J., and Hall, B.D. (2015). Mercury methylation in high and low-sulphate impacted wetland ponds within the prairie pothole region of North America. Environmental Pollution, 205:269–277.

29. Hong, Y., Kim, Y., and Lee, K. (2012). Methylmercury Exposure and Health Effects. Journal Of Preventive Medicine & Public Health, 45(6):353-363.

30. Janssen, S., Schaefer, J., Barkay, T., & Reinfelder, J. (2016). Fractionation of Mercury stable isotopes during microbial Methylmercury production by Iron- and Sulfate-reducing bacteria. Environmental Science & Technology, 50(15):8077-8083.

31. Jansson, J.K., and Tas, N. (2014). The microbial ecology of permafrost. Nature Reviews Microbiology, 12:414–425.

32. Jensen, S., and Jernelov, A. (1969). Biological methylation of Mercury in aquatic organisms. Nature, 223.

33. Johnson, N.W., Mitchell, C.P.J., Engstrom, D.R., Bailey, L.T., Coleman, J.K., and Berndt, M.E. (2016). Methylmercury production in a chronically sulfate-impacted sub-boreal wetland. Environmental Science: Processes and Impacts, 18(6):725–734.

34. Jonsson, S., Skyllberg, U., Nilsson, M., Westlund, P., Shchukarev, A., Lundberg, E., & Björn, E. (2012). Mercury methylation rates for geochemically relevant Hg II species in sediments. Environmental Science & Technology, 46(21):11653–11659.

35. Kim, M., and Zoh, K. (2012). Fate and transport of Mercury in environmental media and human exposure. Journal of Preventive Medicine & Public Health, 45(6):335-343.

36. King, J., Kostka, J., Frischer, M., and Saunders, F. (2000). Sulfate-reducing bacteria methylate Mercury at variable rates in pure culture and in marine Sediments. Applied and Environmental Microbiology, 66(6):2430-2437.

37. Kronberg, R., Tjerngren, I., Drott, A., Björn, E., and Skyllberg, U. (2012). Net Degradation of Methyl Mercury in Alder Swamps. Environmental Science & Technology, 46(24):13144-13151.

38. Kushkevych, I. (2014). Acetate kinase activity and kinetic properties of the enzyme in Desulfovibrio piger Vib-7 and Desulfomicrobium sp. Rod-9 intestinal bacterial strains. The Open Microbiology Journal, 8(1):138-143.

39. Mauro, J., Guimarães, J., and Melamed, R. (1999). Mercury methylation in a tropical macrophyte: influence of abiotic parameters. Applied Organometallic Chemistry, 13(9):631-636.

40. Menon, S., and Ragsdale, S. (1999). The role of an Iron-Sulfur cluster in an enzymatic methylation reaction. Journal Of Biological Chemistry, 274(17):11513-11518.

41. Monperrus, M., Tessier, E., Amouroux, D., Leynaert, A., Huonnie, P., and Donald, O.F.X. (2007). Mercury methylation, demethylation and reduction rates in coastal and marine surface waters of the Mediterranean Sea. Marine Chemistry, 107:49–63.

42. Morel, F., Kraepiel, A., & Amyot, M. (1998). The chemical cycle and bioaccumulation of Mercury. Annual Review Of Ecology And Systematics, 29(1):543-566.

43. Olson, M., Cleckner, L., Hurley, J., Heelan, T., and Krabbenhoft, D. (1997). Resolution of matrix effects on analysis of total and methyl mercury in aqueous samples from the Florida Everglades. *Fresenius' Journal Of Analytical Chemistry*, *358*(3):392-398.

44. Oremland, R., Culbertson, C., and Winfrey, M. (1991). 1991. Methylmercury decomposition in sediments and bacterial cultures: involvement of methanogens and sulfate reducers in oxidative demethylation. Applied Environmental Microbiology, 57:130–137.

45. Orth, J., Thiele, I., and Palsson, B. (2010). What is flux balance analysis? Nature Biotechnology, 28(3):245-248.

46. Pak, K., and Bartha, R. (1998). Mercury Methylation and Demethylation in Anoxic Lake Sediments and by Strictly Anaerobic Bacteria. Applied Environmental Microbiology, 64(3):1013-1017.

47. Parks, J., Johs, A., Podar, M., Bridou, R., Hurt, R., Smith, S., Tomanicek, S., Qian, Y., Brown, S., Brandt, C., Palumbo, A., Smith, J., Wall, J., Elias, D. and Liang, L. (2013). The genetic basis for bacterial Mercury methylation. Science, 339(6125):1332-1335.

48. Pacyna, E., Pacyna, J., Steenhuisen, F., and Wilson, S. (2006). Global anthropogenic mercury emission inventory for 2000. Atmospheric Environment, 40(22):4048-4063.

49. Podar, M., Gilmour, C.C., Brandt, C.C., Soren, A., Brown, S.D., and Crable, B.R. (2015). Global prevalence and distribution of genes and microorganisms involved in mercury methylation. Science Advances, 1500675.

50. Ramlal, P.S., Rudd, J.W.M., and Hecky, R.E. (1986). Methods for measuring specific rates of mercury methylation and degradation and their use in determining factors controlling net rates of mercury methylation. Applied and Environmental Microbiology, 51:110–114.

51. Roskoski, R. (2015). Michaelis-Menten Kinetics. Horse Shoe, NC, USA: Elsevier Inc.

52. Schaefer, J., and Morel, F. (2009). High methylation rates of mercury bound to cysteine by Geobacter sulfurreducens. Nature Geoscience, 2(2):123-126.

53. Schaefer, J., Rocks, S., Zheng, W., Liang, L., Gu, B., and Morel, F. (2011). Active transport, substrate specificity, and methylation of Hg (II) in anaerobic bacteria. Proceedings Of The National Academy Of Sciences, 108(21):8714-8719.

54. Schaefer, J., Szczuka, A., and Morel, F. (2014). Effect of divalent metals on Hg(II) uptake and methylation by bacteria. Environmental Science & Technology, 48(5):3007-3013.

55. Steckling, N., Tobollik, M., Plass, D., Hornberg, C., Ericson, B., Fuller, R., & Bose-O'Reilly, S. (2017). Global burden of disease of Mercury used in artisanal small-scale Gold mining. Annals Of Global Health, 83(2):234-247.

56. Stern, G.A., Macdonald, R.W., Outridge, P.M., Wilson, S., Chételat, J., Cole, A. (2012). How does climate change influence arctic mercury? Science of the Total Environment, 414:22–42.

57. Tchounwou, P., Yedjou, C., Patlolla, A. and Sutton, D. (2012). Heavy metals toxicity and the environment. Molecular, Clinical and Environmental Toxicology, 101:133-164.

58. Widdel, F., and Pfennig, N. (1981). Sporulation and further nutritional characteristics of Desulfotomaculum acetoxidans. Archives Of Microbiology, 129(5):401-402.

59. Yang, Z., Wullschleger, S.D., Liang, L., Graham, D.E., and Gu, B. (2016). Effects of warming on the degradation and production of low-molecular-weight labile organic carbon in an Arctic tundra soil. Soil Biology and Biochemistry, 95:202–211.

60. Zane, G., Yen, H., & Wall, J. (2010). Effect of the Deletion of qmoABC and the Promoter-Distal Gene Encoding a Hypothetical Protein on Sulfate Reduction in Desulfovibrio vulgaris Hildenborough. Applied And Environmental Microbiology, 76(16):5500-5509.

Appendix: Computer Code for the Simulation Model

```
<html>
  <head>
  <script src="https://ajax.googleapis.com/ajax/libs/jquery/3.2.1/jquery.min.js"></script>
  <script src="https://cdn.plot.ly/plotly-latest.min.js"></script>
  <script src="http://code.jquery.com/jquery-1.9.1.js"></script>

  <script>
    function validate(){
      var x=document.forms["form"]["input1"].value;
      var y=document.forms["form"]["input2"].value;
      if(isNaN(x) || isNaN(y)){
        alert("input is not valid")
        return false
      }
      }
  </script>
  <script>
    $(document).ready(function () {
        $('#att1').change(function () {
        $('#temp').fadeToggle();
        });
      });
    $(document).ready(function () {
        $('#att2').change(function () {
        $('#ph').fadeToggle();
        });
```

```
    });
  $(document).ready(function() {
    $('.cat').click(function() {
          $('#merc').show();
          });
     $('.cat1').click(function() {
          $('#merc').hide();
          });
     $('#Form').on("submit", function () {
        $('#res').show();
        });
  });
```

// calling functions required for code to run

```
</script>
</head>
<body>
  <h1> Methyl Mercury Calculator <br>
          <P><font size = "4">Master's Thesis Project by Swetha Kasetty <br>
          swethak.kasetty@gmail.com </font>
          <p>
          <font color="grey"><font size = "4">This model is based on lab studies with pure cultures of <i> Desulfovibrio desulfuricans </i> ND132 and data from literature.<br>
            It is a mathematical approach for analyzing the flow of metabolites through a mercury methylation metabolic network.<br>
              The model calculates methyl mercury (Me-Hg)concentrations and methylation rates for pure culture samples and for <br>environmental samples.
```

This simplified simulation model is a novel application of flux balance model to help with
quantification of Me-Hg in support of management and remediation of harmful mercury emissions.</p>

//adding text and information about the program

</h1>

 Methods

References

Metabolic pathway

<h1>(Click above for more information) </h1>

// adding a link to methods, references etc. A pdf file containing the information is required

<form id='Form' method="POST" action="" name='form' onsubmit="return validate();">

 Enter pyruvate concentration: <input tpye='text' name='input1'>

<input type="radio" name="conc" value="mole"> Moles

<input type="radio" name="conc" value="millimole"> milliMoles

<input type="radio" name="conc" value="micromole" checked> microMoles

<input type="radio" name="conc" value="nanomole"> nanoMoles

<input type="radio" name="conc" value="picomole"> picoMoles

// asking user to input pyruvate conc.

<h1> (Only low concentrations in nanomolar effects Me-Hg rate) </h1>

 Enter Hg(II) concentration: <input type='text' name="input2" >

<input type="radio" name="conc1" value="mole"> Moles

<input type="radio" name="conc1" value="millimole"> milliMoles

```
<input type="radio" name="conc1" value="micromole" checked> microMoles

<input type="radio" name="conc1" value="nanomole"> nanoMoles

<input type="radio" name="conc1" value="picomole"> picoMoles

</b>

<h1><font color="grey"><font size = "2">(Microbes stop methylating at 5 micromoles; Concentrations of 50 micromoles or higher is considered toxic and could lead to cell death)</font></font> </h1><br>
```

// asking user to input Hg (II) conc.

```
<h1> Select your Condition</h1>

<input type="radio" name="molecule" value="glut" checked class='cat' > Glutathione (fumerate reducing condition)

<input type="radio" name="molecule" value="sulf" class='cat1'> Sulfate reducing condition

<input type="radio" name="molecule" value="env" class='cat1'>Environmental

<br><br>
```

// selecting condition

```
<h1>Select output units</h1>

<input type="radio" name="output" value="mole" checked> Moles

<input type="radio" name="output" value="millimole"> milliMoles

<input type="radio" name="output" value="micromole"> microMoles

<input type="radio" name="output" value="nanomole"> nanoMoles

<input type="radio" name="output" value="picomole"> picoMoles

<br><br>
```

// selecting output units

```
<h1>Choose your graph fit</h1>

<input type="radio" name="type" value="linear"> Linear

<input type="radio" name="type" value="poly"> Polynomial <br><br>
```

```
        <input type="checkbox" id="att1" name="att[]" value="temp" checked>
Temperature&#8451
        <input type="checkbox" id="att2" name="att[]" value="ph" checked> pH <br><br>
        <div id='temp'>
          Enter temperature (10-50&#8451): <input type="text" name='tval'><br><br>
        </div>
        <div id="ph">
          Enter pH (Range 4-9): <input type="text" name='pval'><br>
        </div>
                // selecting graph fit



        <br><br>
        <input type='submit'>
      </form>
<div id='res'>
<?php
  error_reporting(0);



  if(isset($_POST['input1']) or isset($_POST['input2'])){


    if($_POST['conc'] == 'mole'){
      $_POST['input1'] = $_POST['input1'] * 1000000;
    }
    elseif($_POST['conc'] == 'millimole'){
      $_POST['input1'] = $_POST['input1'] * 1000;
    }
    elseif($_POST['conc'] == 'picomole'){
```

```
   $_POST['input1'] = $_POST['input1'] * pow(10,-6);
}
elseif($_POST['conc'] == 'nanomole'){
   $_POST['input1'] = $_POST['input1'] * pow(10,-3);
}


if($_POST['conc1'] == 'mole'){
   $_POST['input2'] = $_POST['input2'] * 1000000;
}
elseif($_POST['conc1'] == 'millimole'){
   $_POST['input2'] = $_POST['input2'] * 1000;
}
elseif($_POST['conc1'] == 'picomole'){
   $_POST['input2'] = $_POST['input2'] * pow(10,-6);
}
elseif($_POST['conc1'] == 'nanomole'){
   $_POST['input2'] = $_POST['input2'] * pow(10,-3);
}
```

//Conversion of units

```
$conc_THF=(0.011*$_POST['input1'])/(0.290+$_POST['input1']);

$conc_corrin=($conc_THF*10)/(0.22-$conc_THF);
```

```
    if($_POST['molecule'] == 'glut'){
      $Final_merc=((5.52*pow(10,-6))* $_POST['input2'] *
$conc_corrin)/((0.13*$_POST['input2']) + ( 0.018 * $conc_corrin) + ($_POST['input2'] *
$conc_corrin));
    }
    elseif($_POST['molecule'] == 'sulf'){
      $Final_merc= 3*log10($_POST['input2']);
    }
    elseif($_POST['molecule'] == 'env'){
      $Final_merc=0.0489 * ($_POST['input2']) + 1.222;
    }

    }

  $perc=round(($Final_merc/$_POST['input2'] * 100),12);
    //outconversion

  if($_POST['type'] == 'poly'){

    if($_POST['att'][0] == 'temp'){
      $calcts=(-0.0312*pow(30,2)) + (1.9409 * 30) -17.199;
      $valt = floatval($_POST['tval']);
      $yt=array();
      $xt=range(10,50,2);
      if(!in_array($valt,$xt)){
        array_push($xt,$valt);
      }
```

```
    sort($xt);
    foreach ($xt as $value){
        $val = (-0.0312*pow($value,2)) + (1.9409 * $value) -17.199;
        if($value == $valt){
            $calct=$val;
        }
        array_push($yt,$val);
    }
}

if($_POST['att'][1] == 'ph'){
    $calcps= (-1.4107*pow(7,2)) + (15.775 * 7) -10.807;
    $valp = floatval($_POST['pval']);
    $yp=array();
    $xp=range(3,8,1);
    if(!in_array($valp,$xp)){
        array_push($xp,$valp);
    }
    sort($xp);
    foreach ($xp as $value){
        $val = (-1.4107*pow($value,2)) + (15.775 * $value) -10.807;
        if($value == $valp){
            $calcp=$val;
        }
        array_push($yp,$val);
    }
}
```

```
}
  //Calculation of equations in model

elseif($_POST['type'] == 'linear'){


   if($_POST['att'][0] == 'temp'){
      $calcts=(0.678*30) - 6.6429;
      $valt = floatval($_POST['tval']);
      $yt=array();
      $xt=range(10,50,2);
      if(!in_array($valt,$xt)){
         array_push($xt,$valt);
      }
      sort($xt);
      foreach ($xt as $value){
         if($value >=10 and $value <32 ){
            $val=(0.678*$value) - 6.6429;
            if($value == $valt){
               $calct=$val;
            }
            array_push($yt,$val);
         }
         elseif($value >=32 and $value <=50){
            $val=(-0.7357*$value)+39.074;
            if($value == $valt){
               $calct=$val;
```

```
            }
            array_push($yt,$val);
        }

    }

}

    if($_POST['att'][1] == 'ph'){
    $calcps=(-11 * 7 )+111;
    $valp = floatval($_POST['pval']);
    $yp=array();
    $xp=range(3,8,1);
    if(!in_array($valp,$xp)){
        array_push($xp,$valp);
    }
    sort($xp);
    foreach ($xp as $value){
        if($value >=3 and $value <6){
            $val=(2.8 * $value)+16.9;
        if($value == $valp){
            $calcp=$val;
            }
            array_push($yp,$val);
        }
        elseif($value >= 6 and $value < 7){
            $val = 34;
        if($value == $valp){
```

```
            $calcp=$val;
        }
            array_push($yp,$val);
        }
        elseif($value >=7 and $value <=8){
            $val = (-11 * $value )+111;
            if($value == $valp){
                $calcp=$val;
            }
            array_push($yp,$val);
        }
      }
   }


}

if($calct){
   $rest=($Final_merc*$calct)/$calcts;
   $perct_input=($rest/$_POST['input2'])*100;
}
if($calcp){
   $resp=($Final_merc*$calcp)/$calcps;
   $percp_input=($resp/$_POST['input2'])*100;
}

   if($_POST['output'] == 'mole'){
      $Final_merc = $Final_merc / 1000000;
```

```
    }
    elseif($_POST['output'] == 'millimole'){
       $Final_merc = $Final_merc * 0.001;
    }
    elseif($_POST['output'] == 'picomole'){
       $Final_merc = $Final_merc * pow(10,6);
    }
    elseif($_POST['output'] == 'nanomole'){
       $Final_merc = $Final_merc * pow(10,3);
    }

  $Final_merc=round($Final_merc,16);

  if(isset($_POST['input1']) or isset($_POST['input2'])){

  //Calculation of equations in model

  echo "<h1>Result</h1>";

  echo "<font color = grey >(Since the Me-Hg production is reported per minute in the
glutathione condition, the numbers are expected to be small)</font>";
  echo "<br><br>";
  if($_POST['molecule'] == 'sulf'){
  echo "The final concentration of Me-Hg(II) at default values of 30&#8451 and 7 pH is ".
sprintf('%e',$Final_merc).
    " ".$_POST['output']."<strong> 32 hour incubation; 0.4-0.7 OD at 660nm</strong>";
  }
  elseif($_POST['molecule'] == 'env'){
  echo "The final concentration of Me-Hg(II) at 30&#8451 and 7 pH is ".
sprintf('%e',$Final_merc)." ".$_POST['output']."/g of soil <strong> 7 day incubation</strong>";
```

```
    }
    else{
    echo "The final rate of Me-Hg(II) at 30&#8451 and 7 pH is ". sprintf('%e',$Final_merc)."
".$_POST['output'] ."/min/mg of protein";
    }
    echo "<br><br>";
    echo "The percentage conversion rate of Hg (II) to Me-Hg is ".round($perc,5)."%";
    echo "<br><br>";
    if($_POST['molecule'] == 'sulf'){
    echo "Me-Hg(II) concentration at the input temperature is ".sprintf('%e',$rest)."
".$_POST['output']."32 hour incubation; 0.4-0.7 OD at 660nm";
    }
    elseif($_POST['molecule'] == 'env'){
    echo "The final concentration of Me-Hg(II) at 30&#8451 and 7 pH is ". sprintf('%e',$rest)."
".$_POST['output']."/g of soil; 7 day incubation";
    }
    else{
    echo "The final rate of Me-Hg(II) at 30&#8451 and 7 pH is ". sprintf('%e',$rest)."
".$_POST['output'] ."/min/mg of protein";
    }
    echo "<br><br>";
    echo "Percentage conversion of Hg (II) to Me-Hg at given temperature is
".round($perct_input,5)."%";
    echo "<br><br>";
    if($_POST['molecule'] == 'sulf'){
    echo "Me-Hg(II) concentration at the input pH is ".sprintf('%e',$resp)." ".$_POST['output']."
32 hour incubation; 0.4-0.7 OD at 660nm";
    }
    elseif($_POST['molecule'] == 'env'){
    echo "The final concentration of Me-Hg(II) at 30&#8451 and 7 pH is ". sprintf('%e',$resp)."
".$_POST['output']."/g of soil; 7 day incubation";
```

```
    }
    else{
    echo "The final rate of Me-Hg(II) at 30&#8451 and 7 pH is ". sprintf('%e',$resp)."
".$_POST['output'] ."/min/mg of protein";
    }
    echo "<br><br>";
    echo "Percentage conversion of Hg (II) to Me-Hg at given pH is ".round($percp_input,5)."%";

    echo "<br><br>";
    }

?>
    </div>
    <div id='grapht'></div>
    <script>
        var jxt= <?php echo json_encode($xt); ?>;
        var jyt= <?php echo json_encode($yt); ?>;
        if(jxt != null || jyt != null){
            var trace1={
                x:jxt,y:jyt,type:'scatter'
            }
        }
        var data=[trace1]


    var layout = {
  title: 'Temperature(°C)',
  xaxis: {
    title: 'Temperature(°C)'
```

```
  },
  yaxis: {
    title: '% Me-Hg (II)'
  }
};


      Plotly.newPlot('grapht',data,layout)
    </script>
    <p><p><font size = 4><font color = gray>(Relative % Me-Hg produced at different
temperatures is displayed here; based on Mauro et al., 1999)</font></font></p></p>
    <div id='graphp'></div>
    <script>
      var jxp= <?php echo json_encode($xp); ?>;
      var jyp= <?php echo json_encode($yp); ?>;
      if(jxp != null || jyp != null){
        var trace2={
          x:jxp,y:jyp,type:'scatter'
        }
      }
      var data2=[trace2]


        var layout = {
  title: 'pH',
  xaxis: {
    title: 'pH'
  },
  yaxis: {
    title: '% Me-Hg (II)'
  }
```

```
};


      Plotly.newPlot('graphp',data2,layout)


   </script>

   <p><p><font size = 4><font color = gray>(Relative % Me-Hg produced at different pH is displayed here; Based on Mauro et al., 1999)</font></font></p></p>


</body>

</html>
```

//Reporting results